J Physiol 589.9 (2011) pp 2275–2286

The Journal of Physiology

ATP-mediated glucosensing by hypothalamic tanycytes

Cameron Frayling, Ruth Britton and Nicholas Dale

School of Life Sciences, University of Warwick, Coventry, CV4 7AL, UK

Non-technical summary The hypothalamus contains key neural circuits involved in the control of feeding and energy balance. Stimulated by the inexorable rise of obesity, there has been intense study of these neural circuits. However, the possible role of non-neuronal cells in the brain has not been extensively considered. We now demonstrate that hypothalamic tanycytes, cells that lie at the interface between the ventricular cerebrospinal fluid and the brain parenchyma, respond to both neuron-derived and circulating agents that signal energy status and arousal. Our study therefore suggests that tanycytes should now be considered as active signalling cells in the brain capable of responding to several types of input and having the potential to participate in the control of energy balance and feeding.

Abstract The brain plays a vital role in the regulation of food intake, appetite and ultimately bodyweight. Neurons in the hypothalamic arcuate nucleus, the ventromedial hypothalamic nuclei (VMH) and the lateral hypothalamus are sensitive to a number of circulating signals such as leptin, grehlin, insulin and glucose. These neurons are part of a network that integrates this information to regulate feeding and appetite. Hypothalamic tanycytes contact the cerebral spinal fluid of the third ventricle and send processes into the parenchyma. A subset of tanycytes are located close to, and send processes towards, the hypothalamic nuclei that contain neurons that are glucosensitive and are involved in the regulation of feeding. Nevertheless the signalling properties of tanycytes remain largely unstudied. We now demonstrate that tanycytes signal via waves of intracellular Ca^{2+}; they respond strongly to ATP, histamine and acetylcholine – transmitters associated with the drive to feed. Selective stimulation by glucose of tanycyte cell bodies evokes robust ATP-mediated Ca^{2+} responses. Tanycytes release ATP in response to glucose. Furthermore tanycytes also respond to non-metabolisable analogues of glucose. Although tanycytes have been proposed as glucosensors, our study provides the first direct demonstration of this hypothesis. Tanycytes must therefore now be considered as active signalling cells within the brain that can respond to a number of neuronally derived and circulating transmitters and metabolites.

(Received 8 November 2010; accepted after revision 3 March 2011; first published online 8 March 2011)
Corresponding author N. Dale: School of Life Sciences, University of Warwick, Coventry CV4 7AL, UK.
Email: n.e.dale@warwick.ac.uk

Abbreviations AgRP, agouti related protein; α-MSH, α-melanocyte stimulating hormone; NPY, neuropeptide Y; POMC, proopiomelanocortin; PVN, paraventricular hypothalamic nucleus; VMH, ventromedial hypothalamic nucleus.

DOI: 10.1113/jphysiol.2010.202051

Introduction

The brain plays a vital role in the regulation of food intake, appetite and ultimately bodyweight. Neurons in the hypothalamic arcuate nucleus, the ventromedial hypothalamic nucleus (VMH) and the lateral hypothalamus are sensitive to a number of circulating signals such as leptin, grehlin, insulin and glucose (Routh, 2003; Song & Routh, 2005; Williams *et al.* 2008; Irani *et al.* 2008). These neurons are part of a network that integrates this information to regulate feeding and appetite (Levin & Routh, 1996; Levin, 2006; van den Top & Spanswick, 2006). For example in the arcuate nucleus, the proopiomelanocortin (POMC)-containing neurons activate neurons of the PVN via release of α-melanocyte stimulating hormone (α-MSH) and suppress the drive to feed (Hillebrand *et al.* 2002; Blouet & Schwartz, 2010). Whereas the neuropeptide Y (NPY)/agouti related protein (AgRP)-containing neurons of the arcuate inhibit both the POMC neurons within the arcuate nucleus and the neurons of the PVN thereby promoting feeding (Hillebrand *et al.* 2002; Blouet & Schwartz, 2010).

While there has been much emphasis on the neural circuitry controlling appetite, there is increasing evidence for potential roles by other cells in the brain. Astrocytes respond to alterations in glucose levels by altering their release of lactate and can thus provide fuel for neurons (Parsons & Hirasawa, 2010). Tanycytes line the third and fourth ventricles and are thought to be glial-like in character (Jarvis & Andrew, 1988). Hypothalamic tanycytes express a number of intermediate filament proteins including vimentin (Chauvet *et al.* 1998; Braun *et al.* 2003; Mullier *et al.* 2010), nestin (Wei *et al.* 2002) and in some cases glial fibrillary acidic protein (GFAP) (Chauvet *et al.* 1998; Braun *et al.* 2003; Sanders *et al.* 2004; Rodriguez *et al.* 2005). They have a cell body that contacts the cerebrospinal fluid (Rodriguez *et al.* 2005). In the third ventricle, the ventral tanycytes around the median eminence (called β2 tanycytes) have a known role in the regulation of gonadotropin-releasing hormone (GnRH) secretion (Prevot 2002; Baroncini *et al.* 2007; Ojeda *et al.* 2008; Prevot *et al.* 2010). However, the roles of the more dorsal hypothalamic tanycytes (termed α1 and α2 tanycytes) remain uncharacterised. Intriguingly, their cell bodies have a single process that projects into the brain parenchyma towards neurons of the arcuate nucleus and the VMH (van den Pol & Cassidy, 1982). Tanycytes are the only cells in the rodent brain to contain type D2 deiodinase, which converts T4 thyroxine to the T3 thyroid hormone (Rodriguez *et al.* 2005; Coppola *et al.* 2007). They have been implicated in glucosensing – they contain glucose transporters and hexokinase (Rodriguez *et al.* 2005; Garcia *et al.* 2001, 2003; Sanders *et al.* 2004); nevertheless direct evidence for this role and the nature of any signalling has remained unresolved.

The proximity of tanycytes to the arcuate nucleus, the VMH and the PVN and their location at the interface of the CSF and the brain parenchyma are suggestive of an important physiological role for these enigmatic cells in nutrient sensing and the regulation of feeding and energy balance. We have systematically studied tanycyte signalling via measurement of intracellular Ca^{2+} and demonstrate in this study that they respond to a number of transmitters involved in arousal and feeding. Furthermore they exhibit ATP-mediated responses to glucose when this is applied selectively to their cell bodies suggesting that they may be highly sensitive to the difference of glucose concentration between the ventricular CSF and brain parenchyma.

Methods

Slices

Sprague–Dawley rats (12–18 days old) were humanely killed in accordance with the UK Animals (Scientific Procedures) Act 1986. The brain was rapidly dissected free and placed in ice cold artificial cerebrospinal fluid (aCSF: 124 mM NaCl, 26 mM $NaHCO_3$, 1.25 mM NaH_2PO_4, 3 mM KCl, 2 mM $CaCl_2$, 1 mM $MgSO_4$, 10 mM D-glucose saturated with 95% O_2–5% CO_2) with an additional 10 mM $MgCl_2$. Coronal sections, 300 μM thick, were cut with a vibrating-blade microtome (Microm HM650). The coronal slices were cut in half down the midline taking care not to disturb the lateral walls of the third ventricle. These were placed in normal aCSF at room temperature for 30–60 min before being transferred to a low glucose (0.5 or 1 mM) aCSF (with 9.5 or 9 mM sucrose included to maintain osmolarity). The slices were then continuously maintained in this low glucose solution.

Imaging

Slices chosen for imaging were incubated with fura-2 AM (12.5 μg ml^{-1} with 0.5% DMSO and 0.05% pluronic 127, obtained from Invitrogen) in low glucose aCSF for 60–90 min. This regime resulted in good loading of the tanycyte layer in the walls of the third ventricle. The slices were mounted in a flow chamber and visualised with an Olympus BX51 microscope through a 60× water immersion objective. An Ixon EM-CCD (Andor Technology, Belfast, UK) was used to collect the images. Illumination at 340 and 380 nm was provided by a mercury arc lamp (Cairn Research Ltd, Faversham, UK) and a monochromator (Optoscan, Cairn Research). Metafluor software was used to control the experiments and store the data. Experiments were performed at room temperature, as the fura-2 fluorescence was more stable under these conditions.

Biosensing

Custom ATP (Llaudet *et al.* 2005; Gourine *et al.* 2005), glucose and null biosensors were provided by Sarissa Biomedical Ltd (Coventry, UK) and connected to a potentiostat (Duostat, Sycopel International, Jarrow, UK). The data were collected via an A/D interface and stored on computer for subsequent analysis. The ATP and null biosensors were used as described previously (e.g. Huckstepp *et al.* 2010). In brief, they were placed on the slice next to the tanycyte layer. A puffer pipette was then used to puff in the vicinity of either the ATP or the null biosensor. The null biosensors lack any enzymes for biosensing but are otherwise identical to the ATP biosensor and thus acted as a control for non-specific responses.

Drug applications

Drugs were either applied via the bathing medium (superfusion rate around 4 ml min^{-1}) or via puffs from a patch pipette (pulled on a P97 puller; Sutter Instrument Co., Novato, CA, USA). The concentration of ATP in the patch pipette was 10 mM (in aCSF). For glucose, sucrose and glucose analogues the concentration was either 150 mM or 300 mM. A 300 mM stock solution of the relevant sugar was made in pure H_2O (thus it was isosmotic with aCSF). This was either used directly in the puffer pipette, or diluted 1:1 with aCSF to give an isosmotic 150 mM solution of the relevant sugar or analogue. To estimate the concentration of glucose applied by this method we used a 125 μm diameter disk shaped glucose biosensor and puffed glucose onto the biosensor (from a similar distance to those used with the slices, and in the same chamber at the same flow rate as the slice experiments) and compared the responses from the puffs with those from known concentrations of bath applied glucose. We found that the concentration delivered was proportional to the duration of the puff Fig. 1*A*); with 300 mM in the pipette, the peak concentration ranged between 2 and 10 mM depending on puff duration; whereas with 150 mM glucose in the pipette, the concentration ranged between 1 and 5 mM depending on puff duration. The duration of the elevated glucose in the bath around the biosensor was less than 5 s, before the bath flow washed it away. Repeated puffs delivered a more sustained elevation of glucose without increasing the peak concentration of glucose (Fig. 1*B*). The relationship of Fig. 1*A* was used to estimate the effective dose of glucose delivered in these experiments (reported in text and legends).

MRS2179, MRS2500 and 2MeSADP were obtained from Tocris Bioscience (Bristol, UK); all other chemicals were obtained from Sigma-Aldrich.

Data analysis

Calculation of the emission ratios (F_{340}/F_{380}) was performed with either Metafluor or ImageJ software. Regions of interest (ROIs) around individual tanycytes were drawn and the average pixel intensity within each ROI calculated. The values for these ROIs were then plotted. To assess the magnitude of the changes a pre-response baseline was calculated from the values for the ROIs for at least 10 consecutive images. The maximum change in the ROI

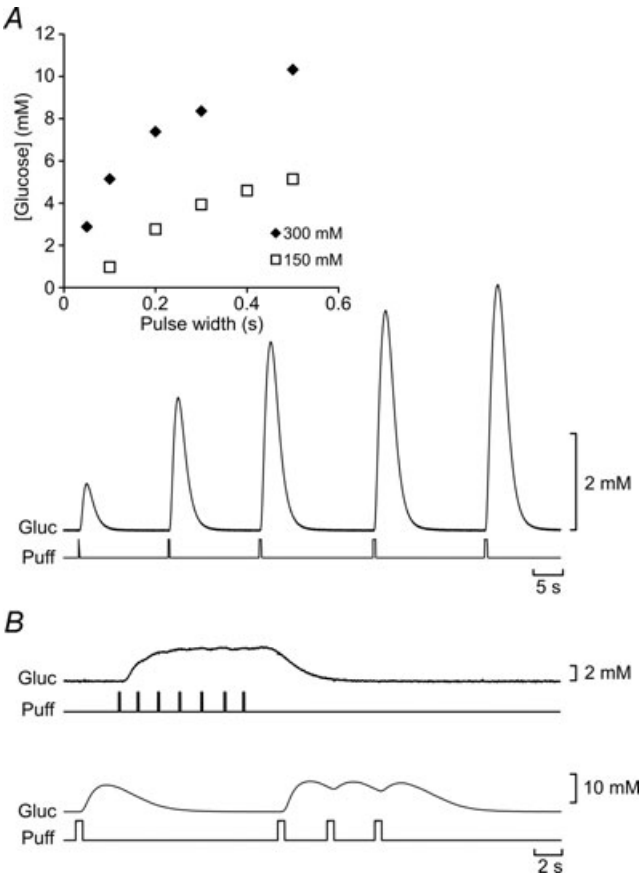

Figure 1. The dependence concentration of glucose delivered via puffer pipettes on the duration of the puff
A, the traces are recordings from a 125 μm disk biosensor for glucose aligned opposite and close to the puffer pipette. The timing pulse of the puffer is shown together with the signal recorded by the glucose biosensor. The concentration of glucose delivered is proportional to pulse with from 0.1 to 0.5 s and depends upon the concentration of glucose within the pipette. The graph shows results from two different pipettes loaded with 150 mM and 300 mM glucose. The traces were obtained with the 150 mM pipette. Both pipettes were from the same series pulled with identical settings on the puller. *B*, repeated puffs of glucose lead to sustained rises in glucose rather than higher glucose concentrations. Top traces show glucose biosensor responses to repeated 0.1 s puffs leading to a steady state concentration of glucose of around 5 mM. The bottom traces show glucose biosensor responses to single and repeated 0.5 s puffs. Glucose at 300 mM in pipette.

intensity was then calculated and the baseline subtracted. For statistical comparison the mean change over all ROIs for an image set was used as a single value.

Analysis of tanycyte waves

To study tanycyte–tanycyte communication via a travelling wave of intracellular Ca^{2+}, 1 μM carboxyfluorescein was included in the puffer pipette along with 10 mM ATP to aid identification of the extent of ATP application along the tanycyte layer. A series of ROIs was drawn along the tanycytes starting from the region of the puff clearly contacted the tanycytes and proceeding in the upstream direction (with respect to bath flow) to regions where there was no drug present. These measurements showed a fluorescence artefact at the time of drug application (0.5 s, thus usually visible only in one frame). In the region where drug was applied, the peak of the response was simultaneous; beyond this region it was visible as a travelling and decrementing wave. The rate of propagation of the wave was determined by the time it took to travel between ROIs.

Statistical comparisons

Comparisons were made with the Mann–Whitney *U* test (independent samples) or Wilcoxon's matched pairs signed ranks test (related samples). Tests of whether responses to agonists were significantly different from zero were made by Student's *t* test and are reported as *P* values immediately following the means ± SEM throughout the text. The frequency of responses to aCSF and glucose puffs was compared by means of the chi squared test.

Results

Tanycytes are readily identifiable at the boundary of the third ventricle with infra-red (IR) imaging. Under low power their contiguous line of cell bodies is evident as a translucent strip along the ventricle wall (Fig. 2*B*). At higher power individual cell bodies can be distinguished along with their inwardly directed processes (Fig. 2*C*). The tanycytes that we recorded from were ventral to the majority of ciliated ependymal cells, but significantly more dorsal than the median eminence and were most probably of the α1 and α2 subtypes (Fig. 2*A* and *B*).

Ca^{2+} signalling in tanycytes

We reasoned that tanycytes might signal via changes in, or waves of, intracellular Ca^{2+} in a manner analogous to the signalling of astrocytes (Volterra & Meldolesi, 2005). We therefore treated hypothalamic slices with fura-2 AM – under these conditions fura-2 readily loaded into the tanycytes, which could be seen as a distinctive line of cells along the ventricle wall (Fig. 2*D*). Exposure of the tanycytes to ATP either focally via puffing from a patch pipette (Fig. 3*A* and *B*) or by bath application (not shown) evoked a robust Ca^{2+} response. When focal application was used this response could travel against the bath flow for some distance away from the site of drug application (Fig. 3*A* and *B*) suggesting that there may be tanycyte to tanycyte spread of the wave. The speed of propagation of this wave was 7.7 ± 0.9 μm s^{-1} ($n = 6$), which is comparable to ATP-mediated Ca^{2+} waves reported in other systems (e.g. Weissman *et al.* 2004; Pearson *et al.* 2005).

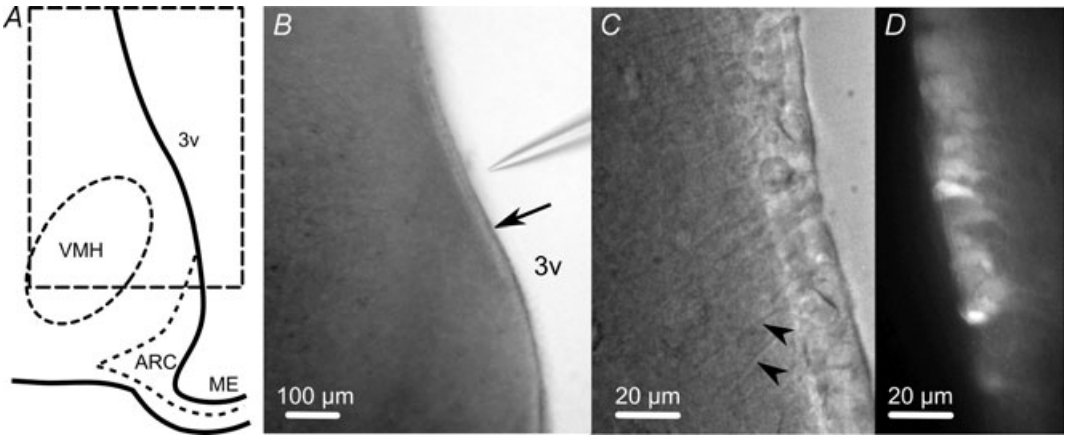

Figure 2. Identification of hypothalamic tanycytes
A, schematic diagram of recording area (bounded by dashed rectangle). VMH, ventromedial hypothalamus; ARC, arcuate nucleus; ME, median eminence; 3v, third ventricle. *B*, low power image (equivalent to dashed rectangle in *A* showing the strip of tanycytes (arrow) and a puffer pipette poised for action. *C*, high power image from a different slice – processes of the tanycytes are visible (arrowheads) and some cilia can be seen at the bottom right hand side of the image. *D*, image at 340 nm of fura-2 loaded tanycytes (from a different slice); their processes are also faintly evident.

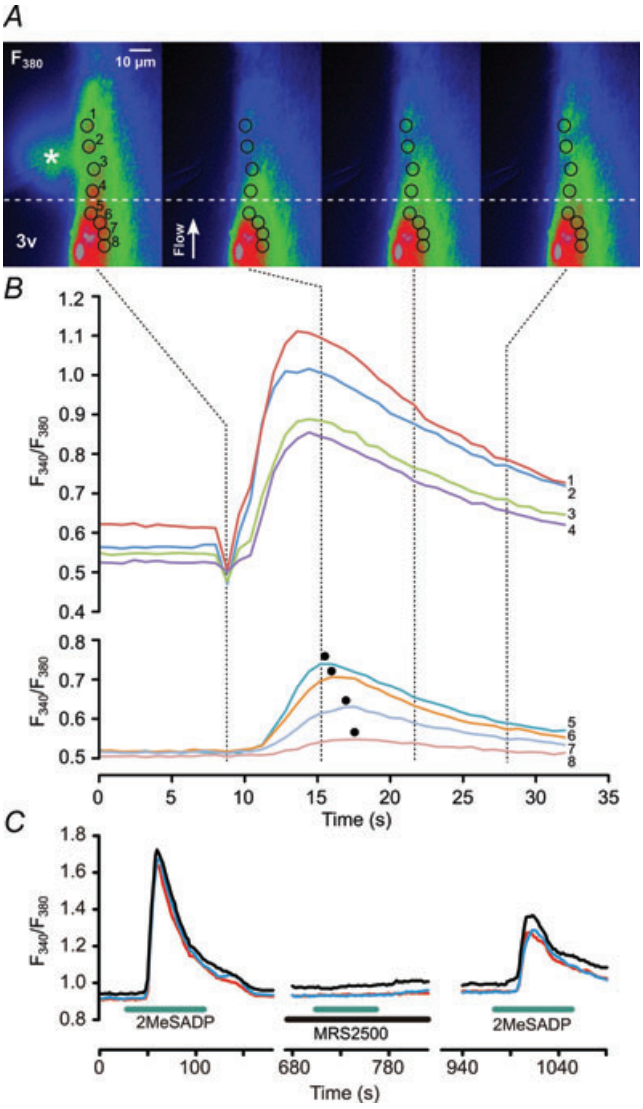

Figure 3. Tanycytes respond to ATP with travelling Ca^{2+} waves via P2Y1 receptors
A, set of fura-2 images (each 6.4 s apart) obtained at 380 nm excitation of the tanycyte layer of the third ventricle (3v). A 0.5 s puff from pipette containing 10 mM ATP (and 1 μM carboxyfluorescein for visualisation) was used to stimulate the tanycytes. The extent of the puff can be seen in the first image (*); the dashed line marks the upstream limit of the puff and 8 ROIs (4 above and 4 below this limit) are marked on the images. The changes in intracellular Ca^{2+} wave at this excitation wavelength are seen as a loss of fluorescence. This loss travelled along the layer of cells and beyond the dashed line (limit of ATP application). The direction of bath flow is indicated by arrow. Thus tanycytes upstream of the pipette exhibited an increase in intracellular Ca^{2+} (ROIs 5–8). *B*, graph of responses in the 8 ROIs shown in *A* calculated as ratios of fluorescence at 340 nm and 380 nm excitation (F_{340}/F_{380}). The top 4 traces (ROIs 1–4) clearly exhibit a fluorescence change (downward deflection) resulting from detection of the carboxyfluorescein in the puffing solution and show a fast and near simultaneous increase in intracellular Ca^{2+}. The bottom 4 traces (ROIs 5–8) show no evidence of the fluorescence change associated with the puff and exhibit a delayed, travelling and decrementing wave of Ca^{2+} increase (speed 8 μm s^{-1}, black circles indicate peak of wave). *C*, fura-2 ratio measurements of the response to bath application of 10 μM 2-methylthio-ADP (2MeSADP, measured with multiple ROIs represented by different coloured lines). The actions of 10 μM 2MeSADP were blocked by 100 nM MRS2500, indicating that the response is mediated by P2Y1 receptors.

The response to ATP was at least partly via P2Y1 receptors as bath application of the agonist 2-methylthio-ADP (2MeSADP) was highly effective at evoking this response (Fig. 3*C*) and responses to 2MeSADP were completely blocked by the highly selective and potent P2Y1 receptor antagonist MRS2500 (mean change in F_{340}/F_{380} 0.83 ± 0.15, in control *versus* 0.03 ± 0.03 in MRS2500, $n = 3$, Fig. 3*C*).

Given their location at the border of the third ventricle and their proximity to structures such as the arcuate nucleus and VMH that integrate a number of signals involved in energy balance, we tested whether tanycytes might respond to transmitters associated with the drive to feed. We found that they responded with increases in intracellular Ca^{2+} to bath application of 10 μM histamine (Fig. 4*A* and *B* mean change in F_{340}/F_{380} 0.22 ± 0.04, $P < 0.01$, $n = 5$) and 10 μM acetylcholine (Fig. 4*C*, mean change in F_{340}/F_{380} 0.14 ± 0.02, $P < 0.01$, $n = 6$).

Bath application of glucose will evoke small Ca^{2+} responses in tanycytes

Following incubation of the slice in aCSF with 1 mM glucose (Methods), application of aCSF containing either 3 or 5 mM glucose for 5 min rarely evoked Ca^{2+} responses in the tanycytes (Fig. 5*A*). However, as tanycytes can respond to transmitters such as histamine and acetylcholine, we reasoned they might act as an integrator of multiple signals related to the state of arousal and energy status. We found that if tanycytes were 'primed' by prior and continued application of 1 μM ACh and 1 μM 5HT (low doses that did not evoke noticeable Ca^{2+} signals), then transitions from 1 to 3 mM bath glucose, or from 1 to 5 mM bath glucose were able to evoke small but readily identifiable changes in intracellular Ca^{2+} (Fig. 5*B*). These changes involved a sustained elevation of intracellular Ca^{2+} often with small transient increases superimposed upon them. The magnitude of the change in F_{340}/F_{380} evoked by 5 mM glucose was 0.034 ± 0.008 ($P < 0.01$, $n = 6$).

Selective stimulation of tanycytes with glucose

However *in situ*, tanycytes normally contact the CSF in the third ventricle, making it plausible that the ventricular surfaces of the tanycyte cell bodies experience different levels of glucose from those present more generally in the brain parenchyma. We therefore utilised patch pipettes to puff glucose onto the tanycyte cell bodies to stimulate them directly without causing generalised activation by glucose of the whole of the slice.

When we puffed glucose onto the tanycyte cell bodies in slices preincubated with aCSF with 0.5 or 1 mM glucose, we observed a spreading Ca^{2+} response of about 20 s in duration (Fig. 6). The mean change in F_{340}/F_{380} to puffs from a pipette containing 300 mM glucose (effective dose at tanycytes in the range 5–8 mM) was 0.27 ± 0.04 ($P < 0.001$, $n = 14$). This was a response specific to the glucose puffs; control puffs from similarly sized patch pipettes filled with aCSF or 300 mM sucrose did not produce these Ca^{2+} responses (effective dose at tanycytes approximately 8 mM Fig. 7, Tables 1 and 2). As a further control to test whether the responses to glucose were dependent on the puff being directed onto the tanycyte somata we performed a series of recordings where we first directly puffed onto the tanycyte cell bodies to demonstrate a glucose response, and then moved the puffer pipette so that it was pointing beyond the tanycyte cell body layer towards the interior of the slice before puffing glucose (effective dose of glucose at tissue approximately 8 mM). This showed that it was important to stimulate the tanycyte cell bodies directly (mean change in F_{340}/F_{380} of 0.21 ± 0.08, $n = 6$) and that simply puffing into the interior of the slice gave either no or very weak responses (mean change in F_{340}/F_{380} of 0.07 ± 0.03, $n = 6$, $P < 0.05$ compared to direct puff, Wilcoxon's matched pairs signed ranks test).

With smaller puffer pipettes filled with 150 mM glucose it was possible to observe responses of a very small number of tanycytes to the glucose puffs, especially if these were repeated over several seconds (effective dose at tanycytes approximately 5 mM, Fig. 8). Puffs of non-metabolisable glucose analogues (2-deoxy-D-glucose and methyl-α-D-glucopyranoside) gave very similar

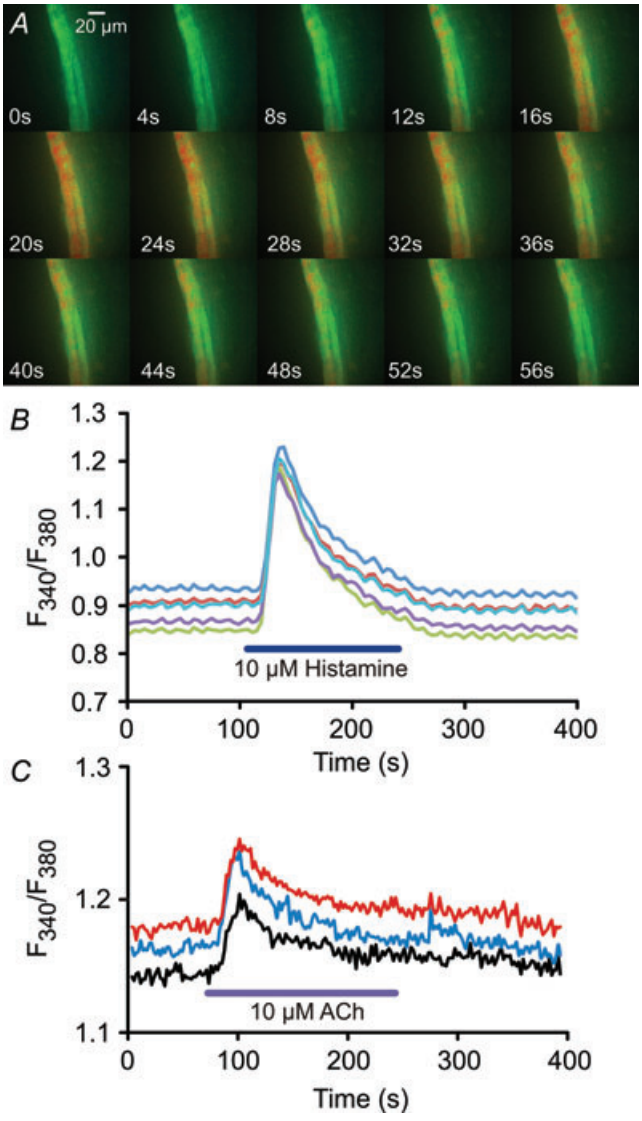

Figure 4. Tanycytes respond to transmitters associated with wakefulness and feeding
A, fura-2 ratio images of the response to bath application of 10 μM histamine. Note the response clearly starts in the tanycyte cell layer (visible at 12 s). *B* and *C*, graphs of the responses (multiple ROIs around tanycytes – coloured lines) to bath applied histamine (above experiment in *A*) and 10 μM acetylcholine.

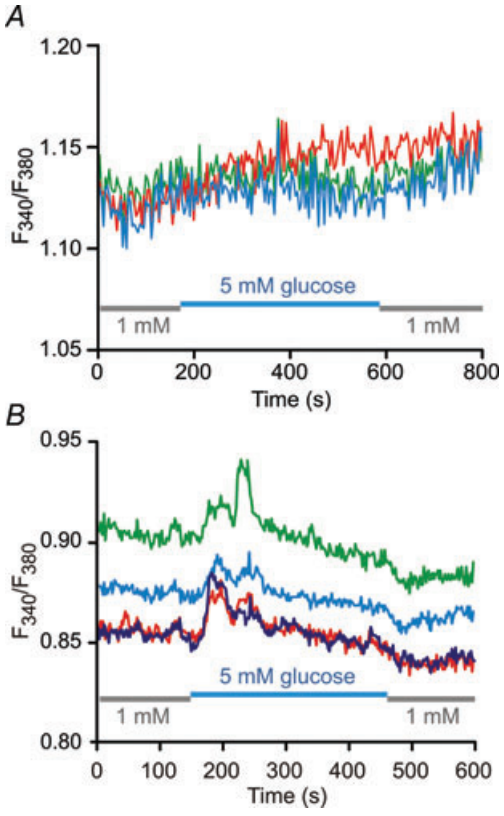

Figure 5. Bath applied glucose can evoke only small Ca^{2+} signals in tanycytes
A, multiple ROI measurements from tanycytes during the application of 5 mM glucose in control aCSF – no responses to glucose are evident. *B*, multiple ROI measurements from tanycytes in a different slice that had been primed with 1 μM acetylcholine and 1 μM 5HT (present throughout the recording) – a small transient response to 5 mM glucose was seen.

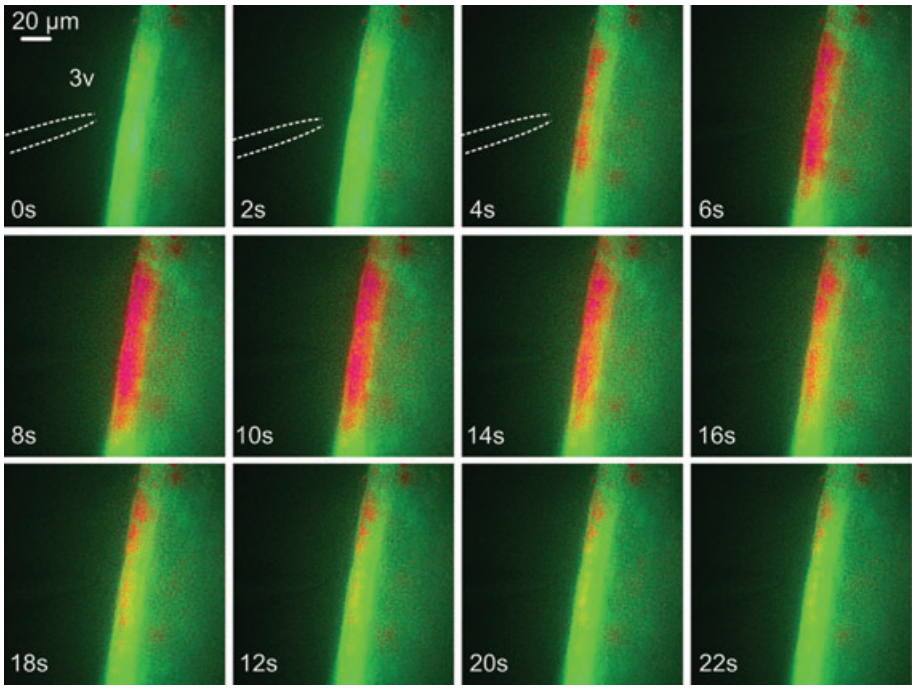

Figure 6. Tanycytes respond strongly to brief puffs of glucose
Fura-2 ratio images showing the response to a puff from a glucose-containing patch pipette (position indicated, 150 mM glucose in pipette, 0.2 s pulse, approximately 3 mM glucose at tanycytes). This evoked a long lasting Ca^{2+} wave in the tanycyte layer; note that the response starts in the tanycyte layer and spreads into the slice.

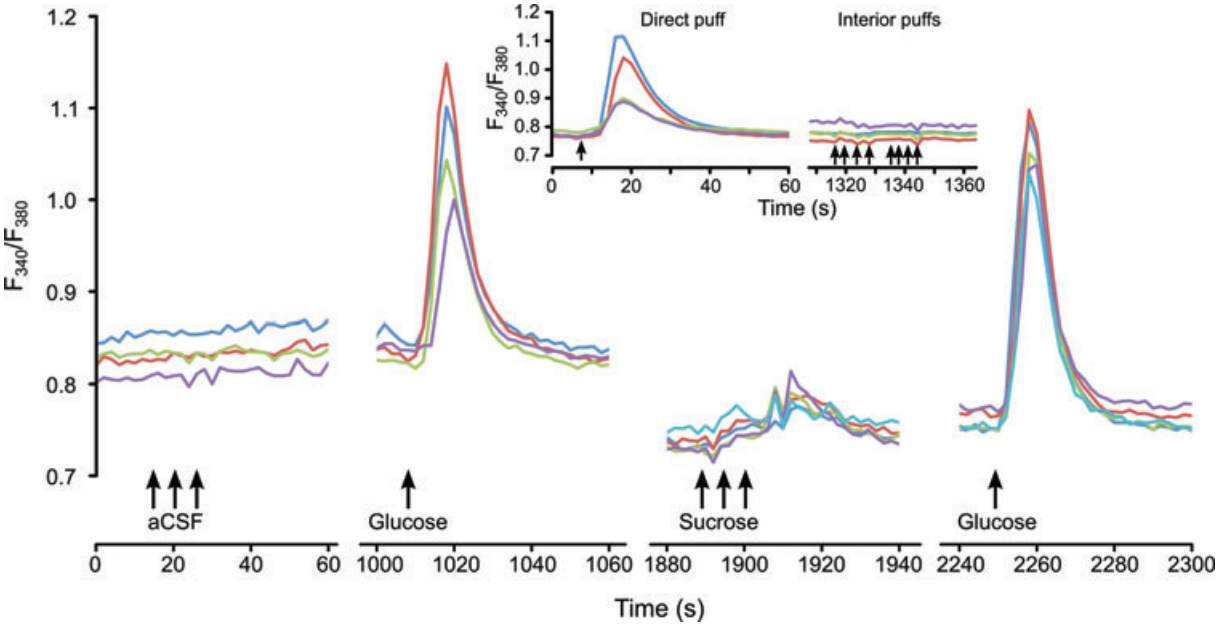

Figure 7. Controls for the specificity of glucose puffs
Multiple ROI measurements (coloured lines) of fura-2 fluorescence from the same slice during a series of puffs of aCSF (arrows), followed by 300 ms puffs from a 300 mM glucose pipette (arrow, approximately 8 mM at tanycytes), a series of 300 ms puffs from a 300 mM sucrose pipette (arrows, approximately 8 mM at tanycytes), followed once more by 300 ms puffs from a 300 mM glucose pipette. All puffer pipettes were pulled from the same series pulled with identical settings on the puller. The inset shows a comparison in the same slice of puffing glucose directly at the tanycyte cell bodies versus puffing, with the same pipette towards the interior of the slice. A single puff (300 ms from a 300 mM glucose pipette, effective dose approximately 8 mM) evoked a clear response, whereas multiple 300 ms puffs from the same pipette moved to the interior did not evoke a response.

Table 1. Interleaved series of control aCSF and glucose puffing (approximately 8 mM at tanycytes) experiments

	Ca^{2+} wave	No Ca^{2+} wave
300 mM glucose	4	9
aCSF	0	25

Statistical analysis (chi squared test) shows that the incidence of Ca^{2+} waves was highly significantly different between glucose and aCSF puffs ($\chi^2 = 8.597$, $P < 0.01$).

Table 2. Interleaved series of glucose and sucrose puffing experiments (each approximately 8 mM at tanycytes) showing the mean change in F_{340}/F_{380} (± SEM)

	Change in F_{340}/F_{380}
300 mM glucose	0.27 ± 0.04, $n = 14$
300 mM sucrose	0.05 ± 0.02, $n = 5$

The two groups are significantly different, $P < 0.002$, Mann Whitney U Test.

responses to glucose (Fig. 9*A* and *B*). The mean change in F_{340}/F_{380} by methyl-α-D-glucopyranoside (300 mM in pipette) was 0.19 ± 0.04 (effective dose at tanycytes approximately 8 mM, $P < 0.01$, $n = 6$) while the mean change for 2-deoxy-D-glucose (150 mM in pipette) was 0.45 ± 0.05 (effective dose at tanycytes approximately 4 mM, $P < 0.001$, $n = 5$).

Glucose responses in tanycytes are mediated by ATP

Given that the Ca^{2+} responses evoked by glucose puffs were highly reminiscent of those evoked by ATP, we tested whether glucose-evoked responses depended upon the activation of P2Y1 receptors. A potent and selective antagonist of the P2Y1 receptor, 100 nM MRS2500, greatly reduced the Ca^{2+} response to glucose (mean change in F_{340}/F_{380} 0.22 ± 0.03 in control, 0.01 ± 0.005 in MRS2500, $n = 8$, $P < 0.01$, Wilcoxon's matched pairs signed ranks test). As the effects of MRS2500 were hard to reverse, we made a few further recordings with the less potent antagonist MRS2179 (and 5 μM) to demonstrate reversible inhibition of the glucose evoked responses (change in F_{340}/F_{380} 0.19 ± 0.09 in control, 0.1 ± 0.08 in MRS2179, $P < 0.05$, $n = 3$, Fig. 9*C*).

Our data suggest that glucose may evoke the release of ATP from tanycytes, which then gives rise to a large Ca^{2+} signal. To test for glucose-evoked release of ATP directly, we placed a miniature ATP biosensor on the tanycyte layer (Fig. 9*D*) while simultaneously puffing glucose onto the tanycytes near the biosensor. We found that glucose did indeed evoke ATP release ($n = 11$) and that in favourable cases the amount of ATP released depended on the proximity of the puffer pipette to the biosensor (Fig. 9*D*). The mean peak concentration of ATP release was 5.2 ± 1.2 μM ($P < 0.01$, $n = 10$) and the duration of the ATP release was 21.4 ± 3 s ($P < 0.001$, $n = 11$). This is a sufficient concentration of ATP to activate P2Y1 receptors and the duration of ATP release is comparable to the duration of the Ca^{2+} response evoked by glucose puffs.

Discussion

Tanycytes are rather poorly studied cells in the CNS. Some authors have termed them neurons (Vigh-Teichmann & Vigh, 1989; Vigh *et al.* 2004); however, electrophysiological studies have shown that they are inexcitable, electrically coupled and thus more glial-like in character (Jarvis & Andrew, 1988). Several different hypotheses for their function have been put forward. For example they have been proposed as mechanosensors (Rodriguez *et al.* 2005) and glucosensitive cells (Rodriguez *et al.* 2005, Garcia *et al.* 2001, 2003; Sanders *et al.* 2004). This last hypothesis has been predicated on the expression of K_{ATP} channels (Thomzig *et al.* 2001), SUR subunits and glucose transporters (Garcia *et al.* 2003) in tanycytes. There is also compelling evidence that tanycytes can act as adult stem cells (Xu *et al.* 2005; Perez-Martin *et al.* 2010). Tanycytes also express proteins necessary for the formation of tight junctions, and may therefore regulate the permeability

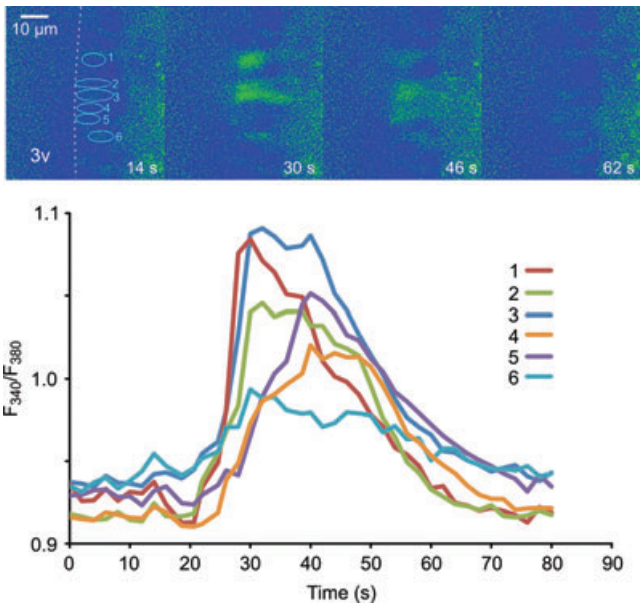

Figure 8. Response from a small group of tanycytes to glucose puffs
Fura-2 ratio images (top) and plot of F_{340}/F_{380} from 6 ROIs (bottom) around 6 distinct tanycytes (ovals, top). The timings on each image relate it to the graph below. The dashed white line indicates the ventricular border of the slice. The individual tanycyte cell bodies exhibit an increase in intracellular Ca^{2+}. Note that the Ca^{2+} signal appears to spread down the tanycyte process. (Response to series of 0.5 s puffs from 150 mM glucose pipette, approximately 5 mM glucose.)

of the barrier between the CSF and brain parenchyma (Mullier *et al.* 2010).

Our results are the first systematic study of rapid signalling by hypothalamic tanycytes. Their signalling capacity seems similar to that of astrocytes – they are sensitive to ATP, which acts via P2Y1 receptors, and are capable of exhibiting relatively rapid increases of intracellular Ca^{2+}. ATP can initiate a travelling Ca^{2+} wave

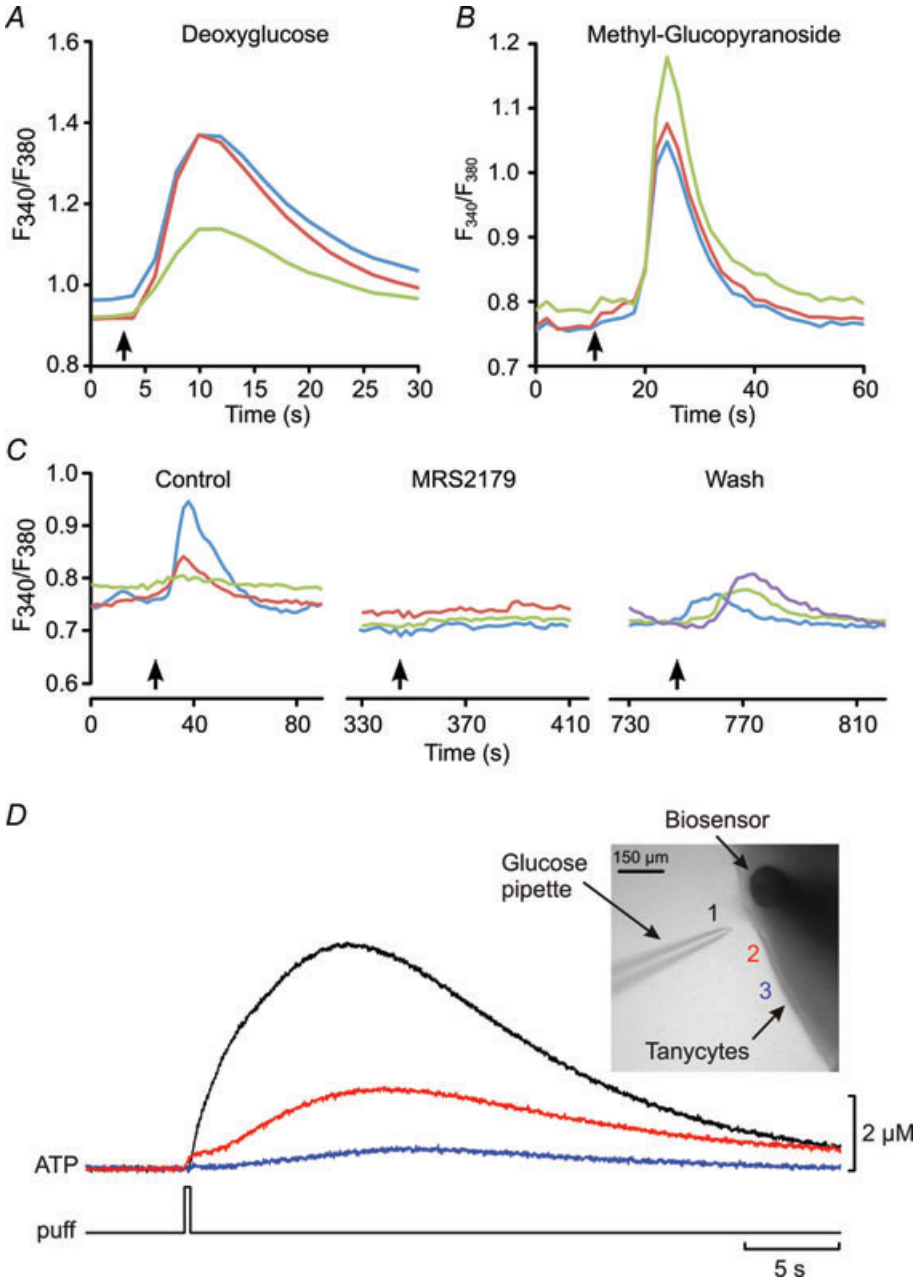

Figure 9. Non-metabolisable glucose analogues evoke Ca^{2+} waves in tanycytes
A and *B*, deoxyglucose (*A*) and methyl-α-D-glucopyranoside (*B*) were effective in evoking substantial Ca^{2+} signals measured by multiple ROIs from tanycytes. *C*, the glucose-evoked Ca^{2+} wave was reversibly blocked by the P2Y1 antagonist MRS2179 (5 μM, bath applied). Arrows indicate timing of puffs from pipettes (*A*, 150 mM deoxyglucose 0.4 s, approximately 4 mM at tanycytes; *B*, 300 mM methyl-α-D-glucopyranoside 0.3 s, approximately 8 mM at tanycytes; and *C*, 300 mM glucose, 0.3 s, approximately 8 mM at tanycytes). Coloured lines represent different ROIs. *D*, tanycytes release ATP in response to glucose. Inset, recording arrangement showing ATP biosensor and glucose pipette; the tanycyte layer can be seen as a translucent strip at the edge of the slice. The numbers indicate the positions of the glucose pipette. Main figure: ATP release evoked by the three positions of the puffer pipette, indicated in the inset, relative to the timing of the puff. Glucose in pipette, 300 mM; 0.3 s puff, approximately 8 mM at the tissue.

along the tanycyte cell body layer. Interestingly Ca^{2+} signalling has been reported in radial glial cells and plays an important role in controlling the proliferation of these stem cells during development of cortex (Weissman *et al.* 2004). It would be interesting to see whether ATP-mediated Ca^{2+} signalling in tanycytes might also be related to their putative role as adult stem cells.

Tanycytes also exhibited Ca^{2+} responses to several other agonists, including histamine and acetylcholine. Interestingly these two transmitters are associated both with wakefulness and the drive to feed (McGinty & Szymusiak, 2003; Meister, 2007; Haas *et al.* 2008). This suggests that tanycytes may be able to integrate several interdependent signals associated with energy status and levels of arousal.

ATP analogues acting via P2Y1 receptors when delivered via infusion into the third ventricle or injected directly into the VMH or lateral hypothalamus will stimulate feeding (Kittner *et al.* 2006), whereas P2Y1 receptor antagonists delivered via the same routes reduce food intake (Kittner *et al.* 2006). Hypothalamic tanycytes are interesting in this light, as our data show that they are sensitive to a number of signals associated with the drive to feed and could represent a cellular source of ATP release in the hypothalamus. Under some circumstances tanycytes may also be stimulated by ATP *in vivo*: during induction of fever, there is a transient rise in ATP concentrations in the third ventricle of the hypothalamus (Gourine *et al.* 2007) to levels sufficient to activate the tanycytes. It is also interesting that tanycytes express NTPDase2, an important enzyme that converts ATP to ADP (Braun *et al.* 2003). The presence of this enzyme is likely to regulate signalling both within tanycytes and potentially between tanycytes and neurons as ATP will activate all P2 receptors, but ADP will only activate certain classes of P2Y receptor.

Our data are the first direct evidence that tanycytes respond rapidly to changes in glucose concentration. With bath application, it was necessary to prime the tanycytes with acetylcholine and 5HT to evoke small responses to changes in glucose. As these transmitters are important in both arousal and feeding, tanycytes may be able to integrate a number of signals associated with energy status and arousal and may act as conditional glucosensors. The effect of priming could either be a direct action on tanycytes (e.g. altering second messenger levels and the phosphorylation state of key proteins) or be a secondary consequence of an action on neurons or astrocytes within the slice (e.g. that prevents them from inhibiting the responses of tanycytes to glucose).

However, even with priming, the responses to bath application of glucose in the tanycytes were very small. By contrast, puffing glucose directly onto the tanycyte cell bodies evoked much larger Ca^{2+} signals and priming was not needed. One reason for this difference could be that puffing allows exposure of the tanycyte cell bodies and brain parenchyma to different levels of glucose, whereas bath application changes the glucose levels uniformly throughout the slice. Puffing application will thus more accurately mimic the case where: (i) cerebrospinal fluid (CSF) levels of glucose may be higher than those in the parenchyma; and (ii) rises in glucose levels in the CSF may initially precede those occurring in the parenchyma. The uniform changes in glucose levels in the entire slice effected by bath application are likely to stimulate many cell types some of which could conceivably release transmitters and modulators to inhibit tanycyte responsiveness to glucose. It is also possible that the tanycytes have a polarity with respect to the molecules involved in glucosensing and must be exposed to differing levels of glucose across their morphology to respond effectively. The recent report by Mullier *et al.* (2010) that tanycytes express tight junction proteins and participate in the permeability barrier between the CSF and parenchyma is especially interesting in the context of our observations.

We have documented the first case of glucose-evoked ATP release. This result suggests that ATP now needs to be considered as an additional potential mediator of glucosensitive responses. Interestingly, ATP has already been identified as a mediator of CO_2 chemosensitivity (Gourine *et al.* 2005). Thus our discovery suggests that ATP signalling might be generally involved in mediating chemosensitivity.

The rapidity of the response to glucose calls into question whether the mechanism of glucosensing in the tanycytes follows the paradigm typified by the pancreatic β cell which has been proposed for glucosensitive neurons (Miki *et al.* 2001). In this the increased production of ATP, resulting from the metabolism of glucose, alters the ATP:ADP ratio and thus the gating of the K_{ATP} channels to give depolarisation. There are difficulties with adapting this paradigm to the responses seen in tanycytes. Firstly non-metabolisable glucose analogues evoke responses in tanycytes; and secondly, it seems unlikely that a brief puff of glucose lasting a few seconds could rapidly change the ATP:ADP ratio. Interestingly, our results with tanycytes have parallels with recent observations of glucosensitivity in neurons of the lateral hypothalamus where non-metabolisable analogues also evoke responses (Gonzalez *et al.* 2008).

One possible hypothesis is that glucose interacts with either a cell surface receptor (Ren *et al.* 2009) or is taken up by Na^+-dependent cotransport (Gonzalez *et al.* 2008). Under the first alternative the G-protein coupled receptor would directly modulate intracellular Ca^{2+} and under the second alternative the resulting elevation of intracellular Na^+ would then cause reversed Na^+/Ca^{2+} exchange and lead to an elevation of intracellular Ca^{2+} on a relatively rapid time scale. The Na^+-dependent transporters can carry a range of glucose analogues (Wright, 2001), but not 2-deoxy-D-glucose (Hediger *et al.* 1995). This substance can permeate through equilibrative glucose transporters

(Uldry & Thorens, 2004). Whatever the initial mechanism for the change in intracellular Ca^{2+}, it would then be sufficient to trigger release of ATP from the tanycytes and subsequent amplification of the Ca^{2+} wave via the P2Y1 receptor.

While tanycytes clearly respond to both circulating and neuronally derived signalling agents, the extent to which tanycytes communicate back to neurons has yet to be established. We have shown that tanycytes can release ATP, and as neurons, including those in the VMH (Kittner *et al.* 2006), express many different ATP receptor subtypes, it is an intriguing hypothesis that tanycytes may modulate neurons of the arcuate nucleus and VMH.

References

Baroncini M, Allet C, Leroy D, Beauvillain JC, Francke JP & Prevot V (2007). Morphological evidence for direct interaction between gonadotrophin-releasing hormone neurones and astroglial cells in the human hypothalamus. *J Neuroendocrinol* **19**, 691–702.

Blouet C & Schwartz GJ (2010). Hypothalamic nutrient sensing in the control of energy homeostasis. *Behav Brain Res* **209**, 1–12.

Braun N, Sevigny J, Mishra SK, Robson SC, Barth SW, Gerstberger R, Hammer K & Zimmermann H (2003). Expression of the ecto-ATPase NTPDase2 in the germinal zones of the developing and adult rat brain. *Eur J Neurosci* **17**, 1355–1364.

Chauvet N, Prieto M & Alonso G (1998). Tanycytes present in the adult rat mediobasal hypothalamus support the regeneration of monoaminergic axons. *Exp Neurol* **151**, 1–13.

Coppola A, Liu ZW, Andrews ZB, Paradis E, Roy MC, Friedman JM, Ricquier D, Richard D, Horvath TL, Gao XB & Diano S (2007). A central thermogenic-like mechanism in feeding regulation: an interplay between arcuate nucleus T3 and UCP2. *Cell Metab* **5**, 21–33.

Garcia MA, Carrasco M, Godoy A, Reinicke K, Montecinos VP, Aguayo LG, Tapia JC, Vera JC & Nualart F (2001). Elevated expression of glucose transporter-1 in hypothalamic ependymal cells not involved in the formation of the brain-cerebrospinal fluid barrier. *J Cell Biochem* **80**, 491–503.

Garcia MA, Millan C, Balmaceda-Aguilera C, Castro T, Pastor P, Montecinos H, Reinicke K, Zuniga F, Vera JC, Onate SA & Nualart F (2003). Hypothalamic ependymal-glial cells express the glucose transporter GLUT2, a protein involved in glucose sensing. *J Neurochem* **86**, 709–724.

Gonzalez JA, Jensen LT, Fugger L & Burdakov D (2008). Metabolism-independent sugar sensing in central orexin neurons. *Diabetes* **57**, 2569–2576.

Gourine AV, Llaudet E, Dale N & Spyer KM (2005). ATP is a mediator of chemosensory transduction in the central nervous system. *Nature* **436**, 108–111.

Gourine AV, Dale N, Llaudet E, Poputnikov DM, Spyer KM & Gourine VN (2007). Release of ATP in the central nervous system during systemic inflammation: real-time measurement in the hypothalamus of conscious rabbits. *J Physiol* **585**, 305–316.

Haas HL, Sergeeva OA & Selbach O (2008). Histamine in the nervous system. *Physiol Rev* **88**, 1183–1241.

Hediger MA, Kanai Y, You G & Nussberger S (1995). Mammalian ion-coupled solute transporters. *J Physiol* **482**, 7S–17S.

Hillebrand JJ, de Wied D & Adan RA (2002). Neuropeptides, food intake and body weight regulation: a hypothalamic focus. *Peptides* **23**, 2283–2306.

Huckstepp RT, id Bihi R, Eason R, Spyer KM, Dicke N, Willecke K, Marina N, Gourine AV & Dale N (2010). Connexin hemichannel-mediated CO_2-dependent release of ATP in the medulla oblongata contributes to central respiratory chemosensitivity. *J Physiol* **588**, 3901–3920.

Irani BG, Le Foll C, Dunn-Meynell A & Levin BE (2008). Effects of leptin on rat ventromedial hypothalamic neurons. *Endocrinology* **149**, 5146–5154.

Jarvis CR & Andrew RD (1988). Correlated electrophysiology and morphology of the ependyma in rat hypothalamus. *J Neurosci* **8**, 3691–3702.

Kittner H, Franke H, Harsch JI, El-Ashmawy IM, Seidel B, Krugel U & Illes P (2006). Enhanced food intake after stimulation of hypothalamic P2Y1 receptors in rats: modulation of feeding behaviour by extracellular nucleotides. *Eur J Neurosci* **24**, 2049–2056.

Levin BE & Routh VH (1996). Role of the brain in energy balance and obesity. *Am J Physiol Regul Integr Comp Physiol* **271**, R491–500.

Levin BE (2006). Metabolic sensing neurons and the control of energy homeostasis. *Physiol Behav* **89**, 486–489.

Llaudet E, Hatz S, Droniou M & Dale N (2005). Microelectrode biosensor for real-time measurement of ATP in biological tissue. *Anal Chem* **77**, 3267–3273.

McGinty D & Szymusiak R (2003). Hypothalamic regulation of sleep and arousal. *Front Biosci* **8**, s1074–1083.

Meister B (2007). Neurotransmitters in key neurons of the hypothalamus that regulate feeding behavior and body weight. *Physiol Behav* **92**, 263–271.

Miki T, Liss B, Minami K, Shiuchi T, Saraya A, Kashima Y, Horiuchi M, Ashcroft F, Minokoshi Y, Roeper J & Seino S (2001). ATP-sensitive K^+ channels in the hypothalamus are essential for the maintenance of glucose homeostasis. *Nat Neurosci* **4**, 507–512.

Mullier A, Bouret SG, Prevot V & Dehouck B (2010). Differential distribution of tight junction proteins suggests a role for tanycytes in blood-hypothalamus barrier regulation in the adult mouse brain. *J Comp Neurol* **518**, 943–962.

Ojeda SR, Lomniczi A & Sandau US (2008). Glial-gonadotrophin hormone (GnRH) neurone interactions in the median eminence and the control of GnRH secretion. *J Neuroendocrinol* **20**, 732–742.

Parsons MP & Hirasawa M (2010). ATP-sensitive potassium channel-mediated lactate effect on orexin neurons: implications for brain energetics during arousal. *J Neurosci* **30**, 8061–8070.

Pearson RA, Dale N, Llaudet E & Mobbs P (2005). ATP released via gap junction hemichannels from the pigment epithelium regulates neural retinal progenitor proliferation. *Neuron* **46**, 731–744.

Perez-Martin M, Cifuentes M, Grondona JM, Lopez-Avalos MD, Gomez-Pinedo U, Garcia-Verdugo JM & Fernandez-Llebrez P (2010). IGF-I stimulates neurogenesis in the hypothalamus of adult rats. *Eur J Neurosci* **31**, 1533–1548.

Prevot V (2002). Glial-neuronal-endothelial interactions are involved in the control of GnRH secretion. *J Neuroendocrinol* **14**, 247–255.

Prevot V, Bellefontaine N, Baroncini M, Sharif A, Hanchate NK, Parkash J, Campagne C & de Seranno S (2010). Gonadotrophin-releasing hormone nerve terminals, tanycytes and neurohaemal junction remodelling in the adult median eminence: functional consequences for reproduction and dynamic role of vascular endothelial cells. *J Neuroendocrinol* **22**, 639–649.

Ren X, Zhou L, Terwilliger R, Newton SS & de Araujo IE (2009). Sweet taste signaling functions as a hypothalamic glucose sensor. *Front Integr Neurosci* **3**, 12.

Rodriguez EM, Blazquez JL, Pastor FE, Pelaez B, Pena P, Peruzzo B & Amat P (2005). Hypothalamic tanycytes: a key component of brain-endocrine interaction. *Int Rev Cytol* **247**, 89–164.

Routh VH (2003). Glucosensing neurons in the ventromedial hypothalamic nucleus (VMN) and hypoglycemia-associated autonomic failure (HAAF). *Diabetes Metab Res Rev* **19**, 348–356.

Sanders NM, Dunn-Meynell AA & Levin BE (2004). Third ventricular alloxan reversibly impairs glucose counterregulatory responses. *Diabetes* **53**, 1230–1236.

Song Z & Routh VH (2005). Differential effects of glucose and lactate on glucosensing neurons in the ventromedial hypothalamic nucleus. *Diabetes* **54**, 15–22.

Thomzig A, Wenzel M, Karschin C, Eaton MJ, Skatchkov SN, Karschin A & Veh RW (2001). Kir6.1 is the principal pore-forming subunit of astrocyte but not neuronal plasma membrane K-ATP channels. *Mol Cell Neurosci* **18**, 671–690.

Uldry M & Thorens B (2004). The SLC2 family of facilitated hexose and polyol transporters. *Pflugers Arch* **447**, 480–489.

van den Pol AN & Cassidy JR (1982). The hypothalamic arcuate nucleus of rat -a quantitative Golgi analysis. *J Comp Neurol* **204**, 65–98.

van den Top M & Spanswick D (2006). Integration of metabolic stimuli in the hypothalamic arcuate nucleus. *Prog Brain Res* **153**, 141–154.

Vigh-Teichmann I & Vigh B (1989). The cerebrospinal fluid-contacting neuron: a peculiar cell type of the central nervous system. Immunocytochemical aspects. *Arch Histol Cytol* **52 Suppl**, 195–207.

Vigh B, Manzano e Silva MJ, Frank CL, Vincze C, Czirok SJ, Szabo A, Lukats A & Szel A (2004). The system of cerebrospinal fluid-contacting neurons. Its supposed role in the nonsynaptic signal transmission of the brain. *Histol Histopathol* **19**, 607–628.

Volterra A & Meldolesi J (2005). Astrocytes, from brain glue to communication elements: the revolution continues. *Nat Rev Neurosci* **6**, 626–640.

Wei LC, Shi M, Chen LW, Cao R, Zhang P & Chan YS (2002). Nestin-containing cells express glial fibrillary acidic protein in the proliferative regions of central nervous system of postnatal developing and adult mice. *Brain Res Dev Brain Res* **139**, 9–17.

Weissman TA, Riquelme PA, Ivic L, Flint AC & Kriegstein AR (2004). Calcium waves propagate through radial glial cells and modulate proliferation in the developing neocortex. *Neuron* **43**, 647–661.

Williams RH, Alexopoulos H, Jensen LT, Fugger L & Burdakov D (2008). Adaptive sugar sensors in hypothalamic feeding circuits. *Proc Natl Acad Sci U S A* **105**, 11975–11980.

Wright EM (2001). Renal Na^+-glucose cotransporters. *Am J Physiol Renal Physiol* **280**, F10–18.

Xu Y, Tamamaki N, Noda T, Kimura K, Itokazu Y, Matsumoto N, Dezawa M & Ide C (2005). Neurogenesis in the ependymal layer of the adult rat 3rd ventricle. *Exp Neurol* **192**, 251–264.

Author contributions

All authors contributed to the design of the study, the collection of the data and the writing of the paper.

Acknowledgements

We thank Dr Marco van den Top, Dr Nina Balthasar and Prof. David Spanswick for helpful comments on earlier drafts of this manuscript and the MRC for support via a Milstein Award. R.B. was a Wellcome Trust vacation scholar.